Bioorganic & Medicinal Chemistry Letters 20 (2010) 594–599

Contents lists available at ScienceDirect

Bioorganic & Medicinal Chemistry Letters

journal homepage: www.elsevier.com/locate/bmcl

Sulfonylureido thiazoles as fructose-1,6-bisphosphatase inhibitors for the treatment of Type-2 diabetes

Eric Kitas *, Peter Mohr, Bernd Kuhn, Paul Hebeisen, Hans Peter Wessel, Wolfgang Haap, Armin Ruf, Jörg Benz, Catherine Joseph, Walter Huber, Ruben Alvarez Sanchez, Axel Paehler, Agnes Benardeau, Marcel Gubler, Brigitte Schott, Effie Tozzo

F. Hoffmann-La Roche Ltd, Discovery Research Basel, CH-4070 Basel, Switzerland

ARTICLE INFO

Article history:
Received 14 October 2009
Revised 17 November 2009
Accepted 17 November 2009
Available online 22 November 2009

Keywords:
Fructose-1,6-bisphosphatase
Allosteric inhibition
Structure–activity studies
X-ray crystallography
Glucose reduction
db/db Mouse model
Aminothiazole bioactivation

ABSTRACT

Sulfonylureido thiazoles were identified from a HTS campaign and optimized through a combination of structure–activity studies, X-ray crystallography and molecular modeling to yield potent inhibitors of fructose-1,6-bisphosphatase. Compound **12** showed favorable ADME properties, for example, $F = 70\%$, and a robust 32% glucose reduction in the acute db/db mouse model for Type-2 diabetes.

Clinical studies have demonstrated that excessive hepatic glucose production (HGP) is responsible for increased fasting blood glucose and significantly contributes to postprandial hyperglycemia.[1] HGP comprises glucose derived from breakdown of glycogen (glycogenolysis) and glucose synthesized from 3-carbon precursors (gluconeogenesis: GNG). A large number of radioisotope studies and several experiments using ^{13}C NMR spectroscopy have shown that GNG can account for up to 100% of the glucose produced by the liver in the non-absorptive state and that the GNG flux is excessive in Type-2 diabetic (T2D) patients.[2] Therefore targeting GNG represents an attractive approach for the control of fasting blood glucose in T2D patients.

Fructose-1,6-bisphosphatase (FBPase) is a key regulatory enzyme of the hepatic GNG pathway and has recently appeared as a target for efficient and safe glycemic control in T2D. It is a tetrameric enzyme that catalyzes the hydrolysis of fructose-1,6-bisphosphate to fructose-6-phosphate and inorganic phosphate. FBPase is regulated synergistically by fructose-2,6-bisphosphate (F2,6P2), a substrate site inhibitor, and AMP, which binds allosterically.[3] Moreover, a second allosteric binding site at the subunit interface has been identified by Wright et al.[4] Based on structural analysis of all three putative FBPase inhibition sites, we judged the allosteric AMP-binding cavity to be the most druggable. Similarly, the phosphonate-inhibitor CS-917 from Metabasis Inc. was also developed as an AMP-binding site inhibitor and was shown in Phase II trials to lower plasma glucose levels in human diabetics. We took the challenge to generate novel AMP-binding site inhibitors that do not require a prodrug approach as used by the phosphonate-inhibitor CS-917.[5]

A HTS campaign was designed to differentiate competitive inhibitors from allosteric ones.[6] The AMP site binders amongst the latter were identified by surface plasmon resonance (Biacore), based on competition with reference compounds.[7] The human liver FBPase crystal structures of different AMP-site inhibitor hit classes were subsequently solved. The complex structures were also used in the selection of an aminothiazole (AT) hit class represented by **1** for further optimization.

The co-crystal structure of **1** with human liver FBPase was solved to a resolution of 2.2 Å. Figure 1 (left panel) reveals that the *p*-tolyl fragment occupies the AMP adenine binding pocket, while the sulfonylurea motif serves as a linker to reach the dyad interface region of two monomers of tetrameric FBPase. In this partly solvent-exposed interface site the two bromothiazole moieties of neighboring ligands interact through π-stacking. A similar binding mode with non-covalent or covalent linkage of two symmetry-related FBPase binding sites has been found previously for sulfonamides[9] and bissulfonylureas,[6] respectively.

* Corresponding author. Tel.: +41 61 6887618; fax: +41 61 6886459.
E-mail address: eric_a.kitas@roche.com (E. Kitas).

0960-894X/$ - see front matter © 2009 Elsevier Ltd. All rights reserved.
doi:10.1016/j.bmcl.2009.11.093

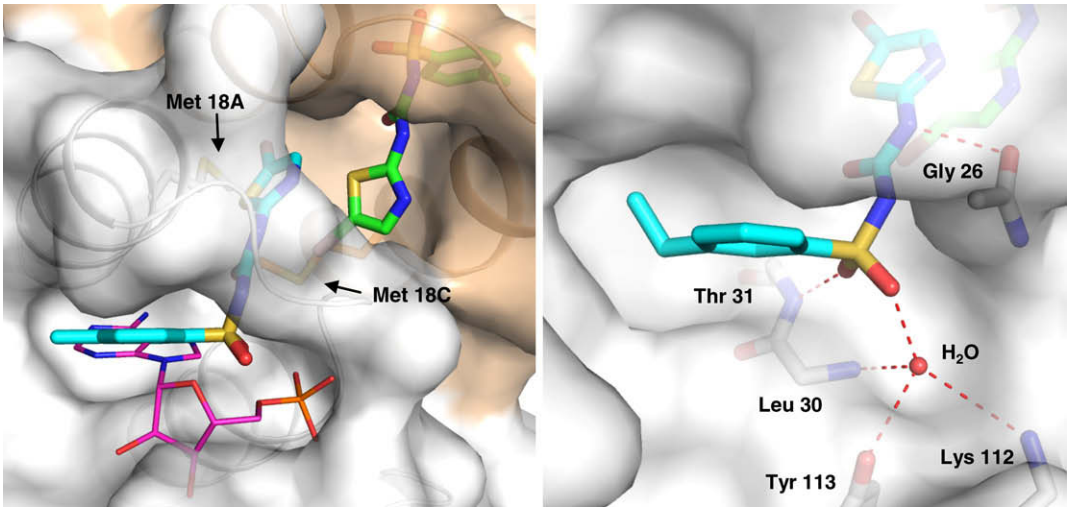

Figure 1. Co-crystal structure of human liver FBPase with **1** (left panel) revealing the binding mode of the sulfonylureido thiazoles (cyan and green). Both the adenine binding site of AMP and the dyad interface region are occupied by the ligand. Protein surfaces of two adjacent FBPase monomers are colored white and gold, respectively. The binding mode of AMP (magenta, PDB id = 1fta) is shown for comparison. The right panel shows a close-up view of the AMP binding pocket of human liver FBPase with **4**. Dashed red lines indicate the H-bonding network of the sulfonylurea motif involving both protein residues and a conserved water molecule.[8]

We extensively explored the SAR for this hit class by considering variations at both ends and by looking for isosters of the sulfonylurea (SU) motif. SAR was built using IC_{50} data of the human and mouse liver enzymes.[10] Efficacy data on mouse hepatocytes were collected in parallel and used for selecting compounds for subsequent in vivo experiments in mouse models.[11]

Table 1
FBPase inhibition: phenyl-substitutions for the adenine pocket[a]

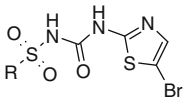

Compound	R	HL IC_{50} (μM)	HL IC_{50} +F2, 6P2 [12](μM)	ML EC_{50} (μM)
AMP		0.44	0.14	—
1	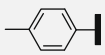	0.92	0.38	118
2		0.31	0.17	23
3		0.35	0.14	19
4		0.23	0.10	32
5		6.4	3.5	>100
6		0.33	0.11	49
7	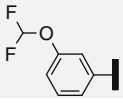	0.21	0.10	24

Table 1 (*continued*)

Compound	R	HL IC_{50} (μM)	HL IC_{50} +F2, 6P2 [12](μM)	ML EC_{50} (μM)
8	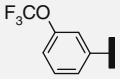	1.0	0.38	>100
9		0.69	0.29	74
10	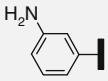	2.1	0.72	>100
11	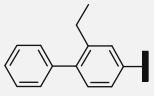	0.15	0.09	63
12	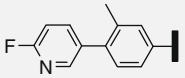	0.13	0.09	10
13	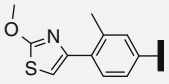	0.32	0.09	62

[a] The HL IC_{50} +F2,6P2 parameter measures the synergistic effect of combining fructose-2,6-bisphosphate (F2,6P2), a substrate site inhibitor, and our allosteric FBPase inhibitors in the enzyme assay; ML EC_{50} values are a measure of efficacy on mouse hepatocytes. Assay conditions have been previously described.[6]

SAR around the adenine binding pocket was in agreement with co-crystal structures where meta-mono-substituents at the phenyl sulfonamide ring were favored, and small substituents (Me, Cl, Et) filling a pocket in the back of the adenine binding site provided an affinity gain of 3–4-fold (Fig. 1, right panel). Larger meta-substituents as in **9,** or the more polar amino derivative **10,** led to loss of affinity. Furthermore, larger substituents, if optimally placed on phenyl, for example, **11**, **12**, were well tolerated and led to increased inhibition of FBPase (Table 1).

We focused on **12** for comprehensive in vitro and in vivo characterization, and its synthesis was undertaken on a multigram

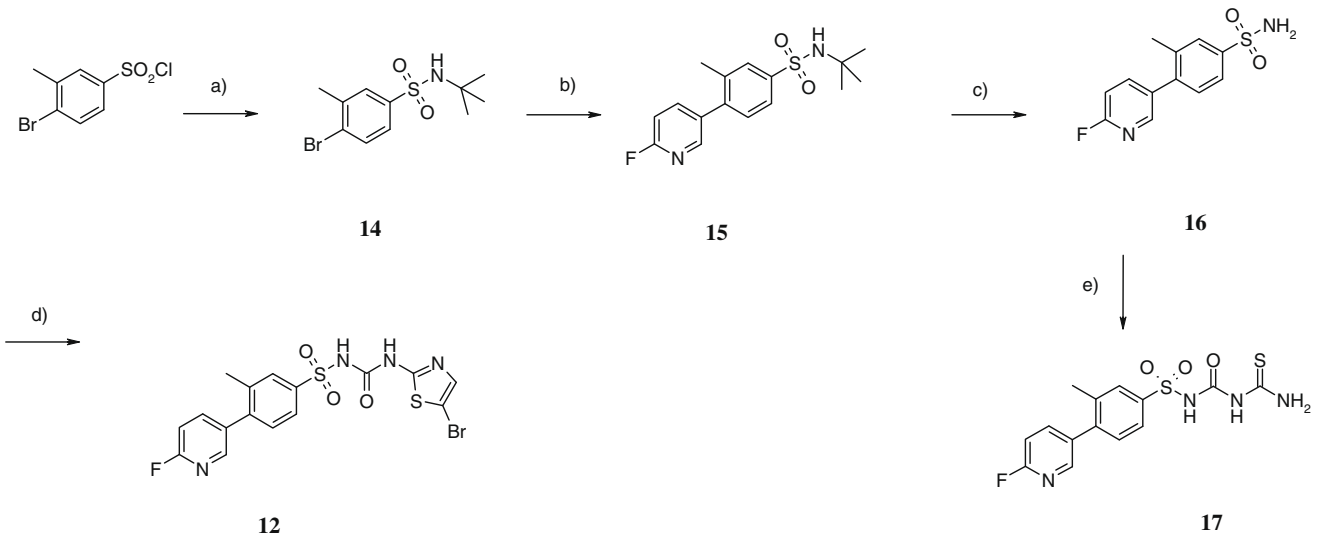

Scheme 1. Reagents and conditions: (a) $tBuNH_2$, DIEA, 84%; (b) 2-fluoropyridine-5-boronic acid, $Pd(PPh_3)_4$, Na_2CO_3, 1,4-dioxane, 86%; (c) 90% TFA, 81%; (d) PhOC(O)Cl, Et_3N, then 2-amino-5-bromothiazole 1.5 equiv, MsOH 1.5 equiv, 68%; (e) as for step (d) but using thiourea as amine.

scale as outlined in Scheme 1. 4-Bromo-3-methylsulfonyl chloride was converted to the aryl *tert*-butyl sulfonamide **14**. This intermediate underwent Suzuki coupling reaction with 2-fluoropyridine-5-boronic acid to furnish **15** in 86% yield. *tert*-Butyl group removal proceeded smoothly using trifluoroacetic acid. The resultant sulfonamide **16** was activated using phenoxy carbonyl chloride and coupled to 2-amino-5-bromothiazole resulting in the desired FBPase inhibitor **12.** Thiourea **17** was prepared as a reference compound for subsequent metabolite studies (see Table 5).

Table 2
FBPase inhibition: heteroaromatic-substitutions for the adenine pocket

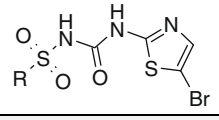

Compound	R	HL IC_{50} (μM)	HL IC_{50} +F2, 6P2 (μM)	ML EC_{50} (μM)
2		0.31	0.17	23
18	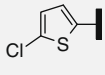	0.44	0.19	92
19	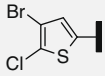	0.23	0.08	87
20	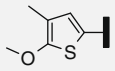	0.15	0.07	24
21	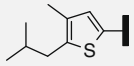	0.04	0.03	13
22	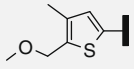	0.22	0.12	10
23	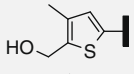	0.31	—	42
24	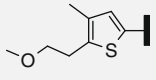	0.09	0.06	5.5
25	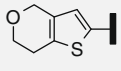	0.53	0.35	27
26	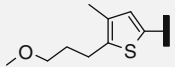	0.09	0.04	3.2

Table 2 (*continued*)

Compound	R	HL IC_{50} (μM)	HL IC_{50} +F2, 6P2 (μM)	ML EC_{50} (μM)
27	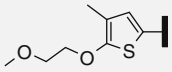	0.31	0.21	12
28	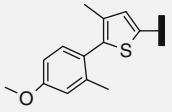	0.07	0.04	19
29	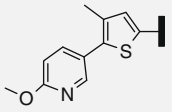	0.15	0.07	34
30	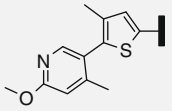	0.06	0.05	9
31	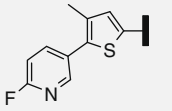	0.06	0.03	9
32	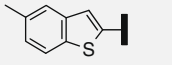	0.09	0.05	18
33	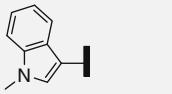	0.39	0.19	14
34	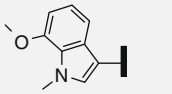	0.07	—	14
35	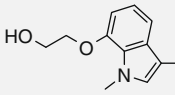	0.10	—	6.3

Table 3
FBPase inhibition: aminothiazole substitutions for the dyad interface

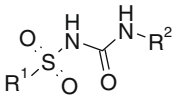

Compound	R^1	R^2	HL IC_{50} (μM)	ML EC_{50} (μM)
24	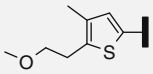	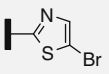	0.09	5.5
36	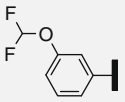	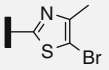	0.17	14
37	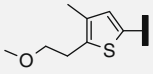	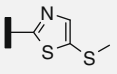	0.18	6.5
38	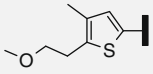	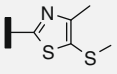	0.18	2.4
39	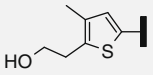	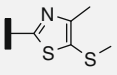	0.07	2.8
40	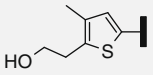	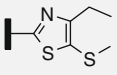	0.08	5.3
41	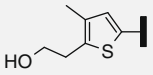	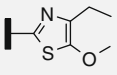	0.26	9.2
42	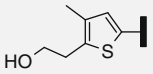	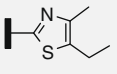	0.41	8.1
43	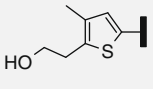	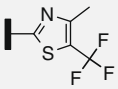	0.3	10
44	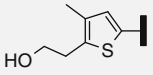	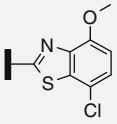	0.04	15
45		H	>100	–
46	H_3C	$(CH_2)_6CONHSO_3CH_3$	>100	–

Besides phenyl sulfonamides our SAR showed that optimally substituted thiophene sulfonamides were well tolerated and led to even improved activity (Table 2). A small β-substituent, for example, methyl, again increased potency by occupying the back pocket in the adenine binding site discussed above. Large α-substituents (methoxyalkyl, substituted aromatic or heteroaromatic) further improved potency and yielded strong inhibitors such as **21, 26** and **30**. The isobutyl substituent of **21** occupies the same binding region as the identical substituent in CS-917 profiting from additional hydrophobic protein–ligand interactions[5] (X-ray structures not shown). Last but not least, biaryls such as benzothiophene **32** and indole **34** also yielded potent inhibitors.

As can be seen from Figure 1, right panel, the sulfonylurea linker shows an exquisite H-bonding network to the protein and a tightly bound water molecule, and has an optimal geometry to protrude into the rather narrow channel linking the adenine and dyad interface binding sites. Not surprisingly, changes to the sulfonylurea moiety (e.g., to acyl urea or acyl sulfonamides, as well as N-alkylations) led to complete loss of affinity. As observed for the covalently linked bissulfonylureas,[6] the phosphate recognition pocket of the AMP-binding site is not occupied by the ligand but by a water molecule, which interacts through four hydrogen bonds with one of the ligand S=O groups as well as Leu30, Lys112, and Tyr113. This is an elegant indirect way to fulfill the binding requirements of the very polar phosphate recognition pocket without the need for strongly acidic ligand functionalities, such as phosphates or phosphonates.

The SAR and X-ray structure analysis of the aminothiazole residue occupying the dyad interface region (Fig. 1, left panel) revealed favorable π-stacking between heteroaromatic residues from ligands bound to adjacent AMP binding pockets as well as strong van der Waals interactions involving 5-substituted polarizable atoms (e.g., Br, S) of adjacent ligands and Met18A and C side chains. These favorable interactions could also be extended to bicyclic aromatic moieties as exemplified by **44**. Small, 4-alkyl substituents were also tolerated and, if combined with hydroxyethyl-substituted thiophene for optimally filling the adenine pocket, resulted in potent inhibitors of FBPase like **39** and **40** (Table 3). Finally, it became evident that both binding regions, that is, the allosteric AMP site and interface region contribute significantly to the binding of the sulfonylureas, as both **45** and **46** were inactive in the FBPase inhibition assay. The R^2 substituent in compound **46** was previously shown to be a favorable motif for the interface site.[6]

The necessary 5-alkoxy- and 5-thioalkoxy-2-aminothiazoles were prepared as summarized in Scheme 2. Bromination of **A**

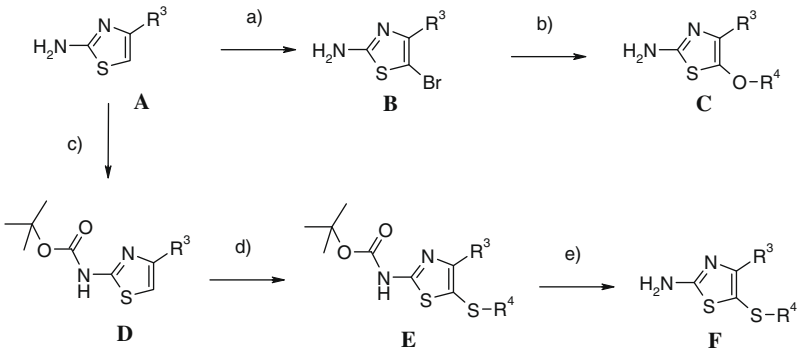

Scheme 2. Reagents and conditions: (a) Br_2, 20% H_2SO_4, 0 °C, 50–70%; (b) $NaOR^4$, 3.5 equiv, HOR^4, 0 °C, 25–50%; (c) BOC_2O, 1.1 equiv, DMAP, 0.1 equiv, $NaHCO_3$, 2.5 equiv, *t*BuOH, 40 °C, 70–80%; (d) *n*BuLi, 2.1 equiv, THF / hexane, −78 °C, then R^4SSR^4, 2.1 equiv, −78 °C to rt, 70–90%; (e) 4 M HCl in 1,4-dioxane, rt, 14 h, 90–100%.

Table 4
ADME profile and mouse PK/PD parameters of **12**

Parameter	Value
Mouse EC_{50} (μM)	10
Cl (human)[a] (μL/min/mg protein)	11.4
Cl (mice)[a] (μL/min/mg protein)	5.1
Cl (mice)[b] (mL/min/kg)	0.1
Vss (L/kg)	0.1
F^c (%)	70
$T_{1/2}$ (h)	8.1
C_{max} plasma (ng/mL)	220,407
Liver-to-plasma ratio	0.6
Glucose reduction after 6 h[d] (% vs vehicle)	32

[a] Microsomal intrinsic clearance.
[b] iv Bolus at 2.5 mg/kg.
[c] Oral gavage at 4.8 mg/kg.
[d] Acute glucose lowering in db/db mouse model [dose = 100 mg/kg po].

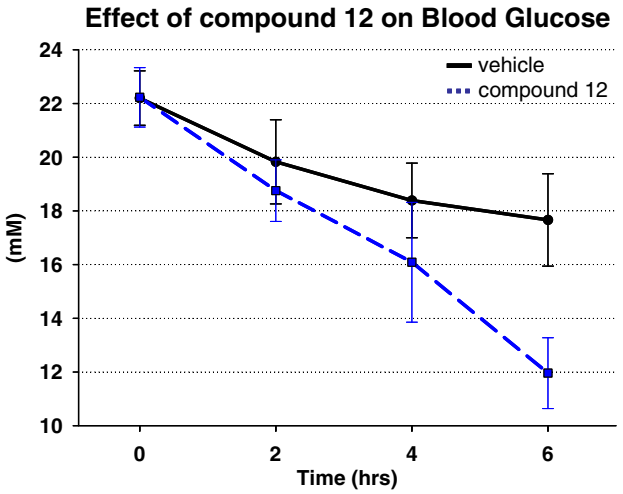

Figure 2. Glucose lowering in db/db mice with compound **12** at 100 mg/kg po versus vehicle.

in aqueous sulfuric acid[13] yielded 5-bromo-analogue **B** which could be transformed directly by nucleophilic aromatic substitution with freshly prepared sodium alkoxide in the corresponding alcohol as solvent already at 0 °C into the rather unstable building blocks **C**. The sulfur-analogues, on the other hand, were preferably synthesized relying on South's method.[14] Mono-BOC-protection under standard conditions afforded **D** in decent yield which was deprotonated twice with *n*BuLi and then quenched with a symmetrical disulfide to give **E**. Smooth removal of the BOC group produced key intermediate **F**. Final assemblage was accomplished as discussed above (Scheme 1, step d).

Having identified potent in vitro inhibitors also showing good cellular efficacy in mouse hepatocytes we selected **12** for further in vivo profiling, as it exhibited good aqueous solubility (465 μg/mL), high membrane permeability (Pe (Pampa)[15] = 3.6×10^{-6} cm/s) and fairly good metabolic stability in microsomes (Table 4). An in vivo pharmacokinetic (PK) study in mice showed low clearance and very low volume of distribution resulting in high plasma exposure, excellent oral bioavailability and a long half-life. This good pharmacokinetic profile resulted in a robust glucose lowering effect upon acute treatment in db/db mice (Table 4 and Fig. 2). Additional in vivo experiments with two other ATs (**27** and **36**) also showed a significant decrease of glucose levels compared to vehicle.[16]

Aminothiazoles suffer from the liability of being oxidized to thioureas, and the latter have been associated with liver toxicity.[17] We have therefore extensively assessed our AT-containing inhibitors for their metabolic reactivity.[18] Formation of thiourea toxophore was determined following compound **12** administration (100 mg/kg po, db/db mice) in an acute efficacy model for blood glucose lowering. In vitro incubations in mouse liver microsomes as well as in vivo samples (plasma and liver taken at 7 h) showed very low content of thiourea metabolite **17** compared to parent as assessed by LC–MS/MS using an authentic standard. Similar observations were made from rat PK experiments (Table 5). Based on the minor formation of **17** in vivo and in vitro, the potential toxicity of thiourea metabolite was not considered to be a major issue for our FBPase inhibitor class. Nevertheless, AT replacements were identified in the lead optimization phase which maintained FBPase inhibition and will be described in a later publication.

The potential for developing FBPase inhibitors not requiring a prodrug strategy has been exemplified by our sulfonylureido series where robust in vivo activity could be demonstrated in the db/db mouse model for Type-2 diabetes.

Table 5
Assessing bioactivation of **12**: thiourea content in hepatic tissue and plasma

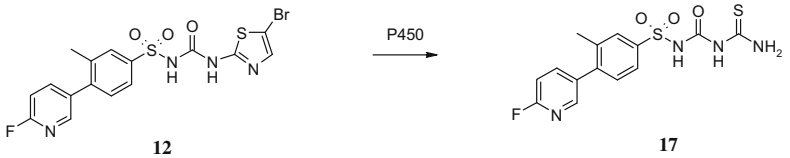

12
in vivo active at
100 mg/kg po db/db mice;
rat/human GSH-adduct clean[16]

17
thiourea toxophore

Sample	% Metabolite **17** (relative to parent)
Rat plasma (single-dose PK profiles)	0.8
Rat liver (single-dose PK @ 8 h)	<1.2
Mouse plasma (PD study 100 mg/kg @ 7 h)	0.8
Mouse liver (PD study 100 mg/kg @ 7 h)	<0.9
Liver microsomes (mouse)	<1.2
Liver microsomes (rat)	<0.5
Liver microsomes (human)	<0.3

Acknowledgements

The excellent technical assistance of Betty Hennequin, Patrick Studer, Stefan Buerli, Thomas Burger, Roland Keller, Rudolf Minder, Lilli Anselm, Stefan Thomi, Tamara Codilupi, Annie Sellam, Anthony Vandjour and Stefan Masur is gratefully acknowledged. Dr. René Wyler is thanked for his encouragement and support.

Supplementary data

Supplementary data associated with this article can be found, in the online version, at doi:10.1016/j.bmcl.2009.11.093.

References and notes

1. DeFronzo, R. A. *Diabetes* **1988**, *37*, 667.
2. Magnusson, I .; Rothman, D. L.; Katz, L. D.; Shulman, R. G.; Shulman, G. I. *J. Clin. Invest.* **1992**, *90*, 1323.
3. Maryanoff, B. E.; Reitz, A. B.; Tutwiler, G. F.; Benkovic, S. J.; Benkovic, P. A.; Pilkis, S. J. *J. Am. Chem. Soc.* **1984**, *106*, 7851.
4. Wright, S. W.; Carlo, A. A.; Carty, M. D.; Danley, D. E.; Hageman, D. L.; Karam, G. A.; Levy, C. B.; Mansour, M. N.; Mathiowetz, A. M.; McClure, L. D.; Nestor, N. B.; McPherson, R. K.; Pandit, J.; Pustilnik, L. R.; Schulte, G. K.; Soeller, W. C.; Treadway, J. L.; Ing-Kae Wang, I.-K.; Bauer, P. H. *J. Med. Chem.* **2002**, *45*, 3865.
5. Erion, M. D.; van Poelje, P. D.; Dang, Q.; Kasibhatla, S. R.; Potter, S. C.; Reddy, M. R.; Reddy, K. R.; Jiang, T.; Lipscomb, W. N. *Proc. Natl. Acad. Sci.* **2005**, *102*, 7970.
6. Hebeisen, P.; Kuhn, B.; Kohler, P.; Gubler, M.; Huber, W.; Kitas, E.; Schott, B.; Benz, J.; Joseph, C.; Ruf, A. *Bioorg. Med. Chem. Lett.* **2008**, *18*, 4708.
7. Huber, W.; Mueller, F. *Curr. Pharm. Des.* **2006**, *12*, 3999.
8. Crystallographic data were collected on beam line X10SA at the Swiss Light Source and coordinates were deposited with the PDB-codes 2WBD and 2WBB for compounds **1** and **4**, respectively.
9. von Geldern, T. W.; Lai, C.; Gum, R. S.; Daly, M.; Sun, C.; Fry, E. H.; Abad-Zapatero, C. *Bioorg. Med. Chem. Lett.* **2006**, *16*, 1811.
10. IC_{50} values are listed as averages of at least two independent experiments.
11. For all our FBPase hit series, we consistently found lower enzymatic activities (5–100-fold) for mouse liver FBPase compared to the human form. This could not be rationalized by the few sequence differences between human and mouse binding sites. It appears that the mouse enzyme generally requires higher concentrations of allosteric AMP site binders to achieve the same allosteric response as the human enzyme. Moreover, mouse EC_{50} values are influenced also by membrane permeability in contrast to human IC_{50} values.
12. The cooperative effect of fructose-2,6-phosphate (F2,6P2) substrate site binding was clearly evident in this series.
13. Ochiai, E.; Nagasawa, H. *Ber. Dtsch. Chem. Ges.* **1939**, *72B*, 1470.
14. South, M. S.; Van Sant, K. A. *J. Heterocycl. Chem.* **1991**, *28*, 1017.
15. For a description of the PAMPA (parallel artificial membrane permeability assay) model, a prediction assay for oral absorption: Kansy, M.; Fischer, H.; Kratzat, K.; Senner, F.; Wagner, B.; Parrilla, I. *Helv. Chim. Acta* **2000**, 447.
16. Old male (13 week) db/db mice on C57BLKS background were block randomized based on blood glucose levels and then orally dosed with 4 mL/kg vehicle (0.3% Tween 80) or compound **12** at 100 mg/kg after 4 h food removal. Blood glucose was monitored with a hand held glucose monitoring device (Roche Diagnostics) at times 0, 2, 4 and 6 h post dose by tail tip bleed. Mice were sacrificed by decapitation immediately after the 6 h time-point and blood and liver were collected for compound exposure and liver glycogen analysis. Glucose results are expressed as a % lowering vs the vehicle group at the same time-point. The statistical analysis of the blood glucose concentration given the experimental design was based on mixed models analysis (random intercepts and random slopes multilevel models). Two models were fitted. The random intercepts proved to be a good representation of the data over random slopes model (based on graphical and information criteria (AIC)). After verifying the model assumptions, hypothesis testing and confidence interval estimation of fixed effects (group, time and their interaction) were carried out, accounting for random effects. Statistical analysis was performed in SAS v8. Blood glucose of mice treated by the compound decrease at a rate of 1.67 (glucose units) per hour (95% CI: 1.28, 2.07) significantly greater than the one observed in the vehicle group: 0.75 (glucose units) per hour (95% CI: 0.38, 1.12).The rate of change of blood glucose over time of mice assigned to the vehicle was significantly lower than that of mice treated with the compound ($p = 0.0014$). Additional data for compounds **27** and **36** also showed significant decrease of glucose (Glc) levels compared to vehicle:

Vehicle	Glc (mM) 0 h	Glc (mM) +2 h	Glc (mM) +4 h	Glc (mM) +6 h
Mean	24.74	20.56	19.07	17.99
Sem	0.93	1.05	1.58	1.47
*Compound **27** (100 mg/kg)*				
Mean	24.00	14.87	11.90	12.54
Sem	0.84	0. 39	0.67	1.37
% vs vehicle		−17	−34	−30

Vehicle	Glc (mM) 0 h	Glc (mM) +2 h	Glc (mM) +4 h	Glc (mM) +6 h
Mean	22.13	21.10	19.24	16.99
Sem	1.11	1.38	1.64	1.16
*Compound **36** (100 mg/kg)*				
Mean	21.57	18.33	15.09	12.57
Sem	1.00	1.54	1.38	1.31
% vs vehicle		8	−11	−26

Vehicle	Glc (mM) 0 h	Glc (mM) +2 h	Glc (mM) +4 h	Glc (mM) +6 h
Mean	22.20	19.83	18.39	17.66
Sem	1.01	1.57	1.39	1.72
*Compound **12** (100 mg/kg)*				
Mean	22.23	18.75	16.09	11.96
Sem	1.11	1.14	2.23	1.32
% vs vehicle		−5	−13	−32

17. Kalgutkar, A. S.; Obach, R. S.; Maurer, T. S. *Curr. Drug Metab.* **2007**, *8*, 407; Kalgutkar, A. S.; Gardner, I.; Obach, R. S.; Shaffer, C. L.; Callegari, E.; Henne, K. R.; Mutlib, A. E.; Dalvie, D. K.; Lee, J. S.; Nakai, Y.; O'Donnell, J. P.; Boer, J.; Harriman, S. P. *Curr. Drug Metab.* **2005**, *6*, 161.
18. Two bioactivation pathways for aminothiazoles resulting in acute liver toxicity through covalent binding have been described.[17] The first is associated with formation of the known toxophore thiourea as discussed in the text. The second pathway involves the formation of reactive thiazolium which could be inferred from glutathione (GSH) trapping experiments. In parallel to the development of the SAR, GSH-adduct formation was assessed for interesting compounds. Within our lead series it became evident that 4- or 5- substitution of the AT ring blocked adduct formation which on the other hand was clearly seen for the 4,5-unsubstituted compound **47**, an inactive compound in the FBPase assay, viz.

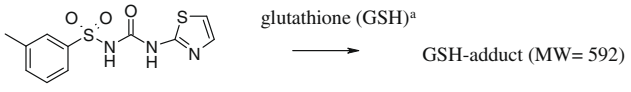

47
(MW =297.4)

[a]Standard test conditions: 10 μM test compound, 1 mg/mL protein, 5 mM GSH, 1 mM NADPH, 60 min incubation.